Palaeontology
The Palaeontological Association
Registered Charity No. 11683330

Evolutionary relationships among bullhead sharks (Chondrichthyes: Heterodontiformes)

Journal:	*Palaeontology*
Manuscript ID	PALA-06-19-4532-OA.R1
Manuscript Type:	Original Article
Date Submitted by the Author:	n/a
Complete List of Authors:	Slater, Tiffany; University of Worcester, School of Science and the Environment; University College Cork, School of Biological, Earth and Environmental Sciences Ashbrook, Kate; University of Worcester, School of Science and the Environment Kriwet, Juergen; University of Vienna, Department of Paleontology
Key words:	Heterodontus, elasmobranch evolution, Paracestracionidae, morphology, bullhead sharks, Late Jurassic

Evolutionary relationships among bullhead sharks (Chondrichthyes: Heterodontiformes)

by TIFFANY S. SLATER[1,2*], KATE ASHBROOK[1], *and* JÜRGEN KRIWET[3]

[1]School of Science and the Environment, University of Worcester, Worcester WR2 6AJ, UK; e-mail: k.ashbrook@worc.ac.uk

[2]*Current address*: School of Biological, Earth and Environmental Sciences, University College Cork, Distillery Fields, North Mall, Cork T23 TK30, Ireland; e-mail: tiffany.slater@ucc.ie

[3] University of Vienna, Department of Palaeontology, Althanstraße 14, Wien 1090, Austria; e-mail: juergen.kriwet@univie.ac.at

*Corresponding author

Abstract: The evolution of modern sharks, skates and rays (Elasmobranchii) is largely enigmatic due to their possession of a labile cartilaginous skeleton; consequently, taxonomic assignment often depends on isolated teeth. Bullhead sharks (Heterodontiformes) are a group of basal neoselachians, thus their remains and relationships are integral to understanding elasmobranch evolution. Here we fully describe †*Paracestracion danieli* – a bullhead shark from the Late Jurassic plattenkalks of Eichstätt, Germany (150–154 Ma) – for its inclusion in cladistic analyses (employing parsimonious principles) using morphological characters from complete †*Paracestracion* and *Heterodontus* fossil specimens as well as extant forms of the latter. Results confirm the presence of two separate monophyletic clades within Heterodontiformes based on predominantly non-dental characters, which show a strong divergence in body morphology between †*Paracestracion* and *Heterodontus* (the latter possessing a first dorsal fin and pectoral fins that are placed more anterior and pelvic fins that are placed more posterior). This study emphasizes the importance of including non-dental features in heterodontiform systematics (as compared to the use of dental characters alone) and supports the erection of the family †Paracestracionidae. Further, phylogenetic analysis of molecular data from five extant species suggests that crown heterodontiforms arose from a diversification event 42.58 Ma off the west coast of the Americas.

Key words: elasmobranch evolution, Late Jurassic, Paracestracionidae, *Heterodontus*, morphology, bullhead sharks

CHONDRICHTHYANS have a very long evolutionary history with their earliest fossil evidence from the Upper Ordovician (Andreev *et al.* 2015). The cartilaginous fishes include the Holocephali, or modern chimaeroids (Maisey 2012), and the Elasmobranchii (sensu Maisey 2012; = Neoselachii of Compagno 1977), i.e. the modern sharks, skates and rays, which experienced rapid diversification in the Jurassic period and are the predominant group of living chondrichthyans (Kriwet *et al.* 2009*a*). Morphological and molecular studies support two major monophyletic shark clades within Elasmobranchii: the Galeomorphii and the Squalomorphii (Carvalho & Maisey 1996; Maisey *et al.* 2004; Winchell *et al.* 2004; Human *et al.* 2006; Mallatt & Winchell 2007; Naylor *et al.* 2012). Although both groups are well represented in the fossil record, their labile cartilaginous skeleton leads to a taphonomic bias towards isolated teeth (Kriwet & Klug 2008). Consequently, much of the early evolutionary history of elasmobranchs is either highly contested or unknown (Klug 2010).

Bullhead sharks (Heterodontiformes) are the most plesiomorphic galeomorphs (Naylor *et al.* 2012), with their remains first appearing in the Early Jurassic (*c.* 175 Ma). Heterodontiforms are therefore among the oldest groups in the fossil record for modern sharks and have the potential to provide insight into early elasmobranch evolution (Thies 1983; Maisey 2012). Several genera of Heterodontiformes seemingly evolved in the Jurassic (Kriwet 2008, Hovestadt 2018): †*Proheterodontus*, †*Palaeoheterodontus*, †*Procestracion* and †*Paracestracion* (all represented by isolated teeth and the last also by complete specimens) disappear from the fossil record before the Cretaceous, while *Heterodontus* underwent further radiation and still occupies our waters today (Kriwet 2008). †*Protoheterodontus* briefly appears in the Campanian (Guinot *et al.* 2013, Hovestadt 2018) but did not make a significant contribution to Late Cretaceous biodiversity.

Bullhead sharks possess a durotrophic littoral ecomorphotype and are characterized by a distinct heterodont dentition with cuspidate anterior teeth to grab invertebrate prey and robust and flattened posterior teeth to crush armoured prey items or small bony fish (Strong 1989; Maia *et al.* 2012). The Eichstätt and Solnhofen areas in southern Germany (and Dover in the U.K.) formed part of an archipelago in the Jurassic that was surrounded by shallow waters of the Tethys Sea (Kriwet & Klug 2008), which likely promoted allopatric speciation in heterodontiforms (Cuny & Benton 1999). Understanding the evolutionary history and past taxonomic diversity of elasmobranchs, however, is encumbered by preservation and collecting biases (Guinot & Cavin 2015).

Completely articulated specimens of elasmobranchs are of utmost importance because they provide abundant anatomical characters for exact taxonomic identification and can inform on morphological, ontogenetic and ecological adaptive changes in their evolution. Here we provide a formal description of †*Paracestracion danieli* – a subadult specimen from the Tithonian of Eichstätt, Germany (150–154 Ma) that was previously identified as a new species (Slater 2016).

Relationships within Heterodontiformes have received surprisingly little attention despite their important phylogenetic position (Maisey 1982, 2012), with recent work including only dental characters (Hovestadt 2018). Anatomical characters from †*Paracestracion* and *Heterodontus* fossils, as well as extant species from the latter, were used in cladistic analyses to examine the evolutionary relationships within heterodontiforms. Taxa based on teeth alone were not included here and, despite recent advances (Hovestadt 2018), their validity remains untested. A taxonomic diversity analysis based solely on extinct and extant heterodontid dentition was, however, performed using data from Hovestadt (2018) and Reif (1976) for comparison. Additionally, the phylogenetic relationships of extant *Heterodontus* were investigated using molecular data from five species. Elucidation of the interrelationships of heterodontiforms will help inform key questions regarding the biodiversity and evolutionary history of heterodontiforms.

MATERIAL AND METHODS

Taxonomic analysis of †Paracestracion danieli

Ultraviolet light was used to expose delicate fossil structures in †*Paracestracion danieli*. High-resolution casts were made of significant anatomical features, such as teeth and placoid scales, which were photographed using a KEYENCE 3D Digital VHX-600 microscope.

Multivariate statistical analysis of heterodontids

Seven distance measurements were taken from †*Paracestracion danieli*, †*P. falcifer* (AS-VI-505), extant juveniles of *H. japonicus, H. zebra, H. portusjacksoni* and two adult *H. japonicus* to identify differences in body shape between genera (Slater *et al.* 2019, table S1, S2). Measurements taken were total body length, length between the anterior and posterior dorsal fin, length between posterior dorsal fin and caudal fin, distance between the pectoral fin and pelvic fin, length between the pelvic fin and anal fin, and widths of the pectoral and pelvic girdle. Distance measurements were corrected for allometry in the software package PAST v.3.20 (Hammer *et al.* 2001) and a Principal Components Analysis (PCA) was performed.

Cladistic analysis of heterodontiforms

Three extant species of *Heterodontus* and fossil specimens of †*Paracestracion*, *Heterodontus* and †*Palaeospinax* – a stem-group representative of Elasmobranchii used to polarize characters (Klug 2010) – were examined to create a robust character matrix (Harvey & Pagel 1991; see Slater *et al.* 2019 for information on specimens used in this study). Morphological trait analysis was carried out using the protocol from Klug (2010). Irrelevant and particularly labile characters were removed and characters specific to Heterodontiformes were added: two cranial (#96, 103), 15 postcranial (#94, 97–102, 104–112), two fin spine (#93, 113), 13 dental (#76–80, 83–84, 86–91) and one denticle character (#92).

A total of 113 characters were used to create a character matrix in the software program Mesquite v.3.51 (Maddison & Maddison 2018). Morphological characters from †*Palidiplospinax* were all coded as [0] (Klug 2010). Soft tissue characters were removed from the matrix prior to analysis and characters that were not applicable to a specimen (such as the presence of molariform teeth in juvenile heterodontids or in the absence of preservation) were coded as [?]. Parsimonious approaches were used in the software program PAUP* v4.0 and 1000 replicates were performed using the heuristic search mode by stepwise addition to obtain bootstrap values (Felsenstein 1985; Swafford 2002). All characters were treated with equal weight. Both ACCTRAN and DELTRAN algorithms were used as they assign character changes as closely as possible to the nodes and tips, respectively (Agnarsson & Miller 2008). Sixty phylogenetically uninformative and/or constant characters were removed (#1–17, 19–26, 28, 30–39, 42–48, 50–51, 53–57, 62, 64–65, 67, 70, 73, 75–76, 104, 112).

Taxonomic diversity analysis

The standing diversity of heterodontiforms was determined for species presented in Hovestadt (2018). Genera of ambiguous systematic position within Heterodontiformes were omitted and 95% confidence intervals (CI) were calculated to obtain a measure for the significance of results. We also consider the stratigraphic distribution of the two dental morphotypes proposed for extant and extinct heterodontiforms by Reif (1976) and Hovestadt (2018).

Molecular phylogeny of extant heterodontids

Homologous NADH2 mitochondrial gene sequences for *Chimaera phantasma* (accession number JQ518719.1), *Torpedo fuscomaculata* (JQ518934.1), *Raja montagui* (JQ518886.1), *Heterodontus galeatus* (JQ518722.1), *H. portusjacksoni* (JQ519033.1), *H. zebra* (KF927894.1), *H. mexicanus* (JQ519166.1) and *H. francisci* (JQ519165.1) were aligned using ClustalW in MEGA v7.0 (Kumar *et al.* 2016). *C. phantasma* was used as the outgroup and a maximum likelihood phylogeny was produced using a GTR+Γ model and an analytical variance estimation with nucleotide substitutions and a strong branch swap filter. Gaps and missing data were treated as complete deletions and 1000 bootstrap replications were executed. A time tree was constructed using a local clock and a minimum and maximum divergence date between Rajiformes and Torpediniformes (187.8–209 Ma) for calibration (Inoue *et al.* 2010; Aschliman *et al.* 2012).

GEOGRAPHICAL AND GEOLOGICAL SETTING

†*Paracestracion danieli* (PBP-SOL-0005) was excavated from the Solnhofen limestone (ca. 153 Ma, early Tithonian, Late Jurassic) near Eichstätt (South Germany; Fig. 1). The fossil-yielding layers consist of finely laminated and strongly silicified calcarenites and calcisiltites (for information about the geology and geography of this area see Kriwet & Klug 2004).

Institutional abbreviations. BSPG, Bayerische Staatssammlung für Paläontologie und Geologie Munich, Germany; JME, Jura Museum Eichstätt, Germany; SMNS, State Museum of Natural History Stuttgart, Germany; PBP-SOL, Wyoming Dinosaur Center, USA.

SYSTEMATIC PALAEONTOLOGY

Superclass CHONDRICHTHYES Huxley, 1880

Class ELASMOBRANCHII Bonaparte, 1838

Cohort EUSELACHII Hay, 1902

Subcohort NEOSELACHII Compagno, 1977

Superorder GALEOMORPHII Compagno, 1973

Order HETERODONTIFORMES Berg, 1940

Family PARACESTRACIONIDAE

LSID. urn:lsid:zoobank.org:act:XXXXXXXXX

Genus †PARACESTRACION Koken, in Zittel, 1911

Type species. †*Cestracion falcifer* Wagner, 1857 (BSPG AS-VI-505); lower Tithonian of Solnhofen, South Germany.

†*Paracestracion danieli*

Figure 2

Derivation of name. Named in honour of J. Frank Daniel for his work on the endoskeleton of extant heterodontiform sharks.

Holotype. PBP-SOL-0005, complete specimen preserved in part and counterpart.

Diagnosis. †*P. danieli* is characterized by the following combination of plesiomorphic and autapomorphic (indicated by an asterisk) morphological traits: labial ornamentation on anterior teeth; absence of distal curvature in parasymphyseal teeth; pectoral girdle positioned at the 12^{th} vertebra*; and first dorsal fin spine placed at the 32^{nd} and 33^{rd} vertebrae*.

Description. The part and counterpart of †*P. danieli* display organic preservation of the body shape and a complete and fully articulated cartilaginous skeleton (Fig. 2A–B). The paired fins are represented by a single fin each: the pectoral fin is ovular in shape (i.e. possesses no distinct margins) and is most broad near its trailing edge, while the pelvic fin – ventral to the anterior dorsal fin and abutting the pectoral fin – is pointed at both its apex and free rear tip and has an anterior and posterior margin of similar length. The anterior dorsal fin (height, 23 mm; length, 40.4 mm) is larger than the posterior (height, 25.9 mm; length, 30.2 mm) but both possess a rounded apex and a gently curved posterior margin. The anal fin is ventral to the posterior dorsal fin, is its own length to the caudal fin and is pointed at its apex. A pointed ventral tip joins the pre- and postventral margin of the caudal fin, with the postventral margin extending dorsocaudally to a ventral posterior tip. The dorsal lobe predominates the caudal fin, whereby the upper postventral margin continues anterodorsally to a broad subterminal notch. The posterior margin and the dorsal posterior 'tip' are rounded and possess no distinct boundaries.

A dense layer of denticles obstructs the view of the neurocranium. The hyomandibula, hyoid and branchial apparatus are embedded in sediment. Segments of the Meckel's cartilage join at the symphysis to form a bulbous rostrum and then extend in a posterolateral fashion (Fig. 2C). One mandible segment is fully exposed in lateral view and maintains a similar height along its entire length; the posterior end does not possess a strong process but is negatively cambered (i.e. the ventral margin extends more laterally than the dorsal margin) before it curves dorsally to form the quadrato-mandibular joint. Features of the palatoquadrate are obscured by sediment. Two dorsal fin spines are positioned directly anterior to each dorsal fin (Fig. 3A–B). The posterior fin spine is larger and more recurved than the anterior and the caps of each bear no tuberculation. Skeletal features such as the propterygium, mesopterygium and metapterygium are visible, however much of their features are embedded in the sediment. Supraneural elements are present and are along the posterior end of the caudal fin.

Exposed teeth on the Meckel's cartilage are preserved *in situ* and are symmetrical and possess a gentle slope. Three small, lateral cusps flank each side of a large, central cusp – all of which possess distinct vertical striations on their labial face (Fig. 2D–F). The pair of cusps most proximal to the central cusp are well developed when compared to the other cusplets. The cusps are not lingually bent and the lateral and posterior teeth are not distally inclined. Anterior teeth are taller than they are wide and exhibit a slightly convex basal labial edge that juts out over the crown/root junction (Fig. 2E–F). Lateral teeth are wider than they are tall, and the basal labial edge is less prominent than in anterior teeth (Fig. 2D). No molariform teeth are present, which supports that the specimen is subadult. The root is gently curved in basal view and the vascularisation is of the holaulacorhize type. Single, circular nutritive foramina are located in the centre of a nutritive groove, which divides the root into two lobes (Fig. 2G). No nutritive foramina are visible on the lateral faces of the root lobes.

The most rostral part of the cranium is densely covered in denticles that are preserved in apical view and have a slightly convex crown surface and a wide posterior margin that gently tapers to a rounded anterior tip (Fig. 2H). Denticle crowns on the rest of the cranium possess (in apical view) a delicate mid-ridge and an arrow-like morphology that is nearly as wide as it is long (Fig. 2I); the ventral side of the body is flanked with denticles of similar morphology but are longer than they are wide (and thus are more pointed at their apex) and have a more prominent mid-ridge in apical aspect (Fig. 2J). Denticles along the anterior margins of the paired fins are again arrow-like in shape but have a weak mid-ridge and a much shorter ‘stem’ than cranial and ventral denticles (Fig. 2K). Many dorsal denticles possess the same morphology as those on the ventral side of the body; some, however, are thorn-like in apical view (Fig. 3C). Anterior to the fin spines are dorsal thorns, which – unlike denticles – sit perpendicular to the body, are slightly concave in lateral view and have a broad base that tapers to a sharp, recurved apex (Fig. 3D).

Occurrence. Late Jurassic (Tithonian, ca. 153 Ma).

RESULTS

Comparison and multivariate statistical analysis of meristic characters

†*Paracestracion danieli* is characterized by seven cusps in anterior teeth at a body length of 225 mm while the holotype of †*P. falcifer* (AS-VI-505) exhibits a single cusp in anterior teeth at a body length of 400mm (Fig. 4). The position of various features along the body column (e.g. at the n^{th} vertebrae) are markedly different between †*P. danieli* and †*P. falcifer*: the dorsal fin spines in the former (anterior: 32^{nd}–33^{rd}; posterior: 62^{nd}–63^{rd}) – as well as the pectoral and pelvic girdle (12^{th} and 32^{nd}, respectively) – are placed more posterior along the body when compared to †*P. falcifer* (anterior fin spine: 23^{rd}–24^{th}; posterior fin spine: 43^{rd}–44^{th}; pectoral and pelvic girdle: 10^{th} and 24^{th}, respectively; Slater 2016, table 1). This is confirmed by multivariate statistical analysis, which reveals that the distance between the pectoral and pelvic fins accounts for the majority of the variation (PC1=78.9%) in body shape between †*P. danieli*, †*P. falcifer* as well as extant species of *Heterodontus*: the distance between the posterior dorsal and caudal fin (PC2) explain 15.9% of the variation (Fig. 5).

Cladistic analysis of heterodontiforms

The cladistic analysis produced one most parsimonious tree with a tree length of 61, a consistency index of 0.9016 (indicating a low amount of homoplasy in the dataset) and a retention index of 0.9062 (indicating that the proportion of terminal taxa retaining the character identified as a synapomorphy is high). Unless specified, characters were assigned to nodes and terminal taxa by both ACCTRAN and DELTRAN optimizations. Results from our analysis support two monophyletic groups, a clade that includes †*Paracestracion* species and one that contains extinct and extant forms of *Heterodontus* (Fig. 6).

Characters supporting the monophyly of node B are the presence of a root shelf that surrounds the entire circumference of the tooth (likely anchoring them in the mucosal tissue), pelvic fins that are ventral to the first dorsal fin and, as assigned by ACCTRAN optimization, abutting the pectorals (Fig. 6). The vertebrae above which the first dorsal fin spine is inserted is considered an autapomorphic character for †*P. viohli,* †*P. falcifer* and †*P. danieli* (22–23rd, 24–25th and 32–33rd vertebrae, respectively).

Node C is characterized by pelvic fins that abut the pectorals and seven cusps on the symphysial teeth as a juvenile, which are both supported by DELTRAN optimization. Specimen SMNS 11150 is identified as a separate species from †*P. falcifer* due to the presence of five cusps on its anterior teeth as a juvenile (ACCTRAN optimization; Fig. S1). †*Paracestracion viohli* (JME Sha 728) is characterized by ornamentation on the lingual tooth crown face and a lack thereof on the labial face in anterior teeth.

Node D features dorsal thorns (DELTRAN optimization) and an absence of distal curvature in the parasymphysial teeth of juveniles. †*Paracestracion danieli* features an additional two characters: a pectoral girdle at the 12th vertebra and the aforementioned position of the first dorsal fin spine.

Node E identifies a monophyletic clade that is supported by a low number of tooth families (≤21) (ACCTRAN optimization), an absence of labial tooth crown ornamentation in anterior teeth, an anal fin that is more than its own length in distance to the caudal fin and a pectoral girdle positioned at the eighth vertebrae. †*Heterodontus zitteli* features accessory cusplets that are nearly the same height as the central cusp and – as in †*P. danieli* – dorsal thorns (DELTRAN optimization) and seven cusps on the anterior teeth (DELTRAN optimization).

Node F features an absence of a horizontal root on the basal face of anterior teeth, labial faces of the crown that jut out over the crown/root junction, anterior teeth with a convex labial face, absence of a cylindrical central cusp, presence of a medio-lingual protuberance, and an absence of fin spine tuberculation. Additional characters are identifiable when ACCTRAN optimization is used: an anal fin that is posterior to the second dorsal fin, absence of dorsal thorns, pectoral fins that are entirely situated anterior to the first dorsal fin, and a high number of vertebral centra. DELTRAN optimization also identifies a low number of tooth rows to this node. †*Heterodontus canaliculatus* is recognized by ACCTRAN as having three cusps in adult anterior teeth.

Node G is exclusive to extant *Heterodontus* and shows a relationship between species occupying shallow waters off of the coasts of Australia and the east coast of Asia. Characters for node G include: two root lobes are inclined and join in the midline of the lingual side of the tooth, broad molariform teeth with no median crest on the cutting edge in adults, an anal fin that is posterior to the second dorsal fin, pectoral fins that are not situated anterior to the first dorsal fin, a low number of vertebrae and a single cusp in adult anterior teeth (the last of which is supported by DELTRAN optimization). *Heterodontus portusjacksoni* has enameloid ridges on molariformes, a less pronounced supraorbital crest, and five cusps in juvenile anterior teeth (the last is supported by ACCTRAN optimization). *H. japonicus*, conversely, has seven cusps in juvenile anterior teeth.

Taxonomic diversity of heterodontiforms

Analysis of data from Hovestadt (2018) shows that the standing taxonomic diversity of fossil heterodontiforms increased from the Early to the Late Jurassic, followed by a 1.7% decrease in species across the Jurassic/Cretaceous boundary (Table 1). The Late Cretaceous represents 26.3% of the total extinct and extant taxonomic diversity for heterodontiforms, with the Cenomanian accounting for most species. Further, an 8.8% decrease in species standing diversity occurs across the K/Pg boundary but is not significant. The Palaeogene represents 17.5% of the total diversity of fossil and extant heterodontiforms, while the Neogene represents 12.3%. Three and six extant species display dental structures of morphotype 1 and 2, respectively.

Molecular phylogeny of extant Heterodontus

Results indicate that *H. francisci* – originating ca. 42.58 Ma – is basal to all other extant heterodontids included in our analysis and that *H. mexicanus* and *H. zebra* diverged from *H. francisci* ca. 27.67 Ma and 9.22 Ma, respectively (Fig. 7). *H. portusjacksoni* and *H. galeatus* are shown to have diverged from each other 7.14 Ma. The low bootstrap support value, however, indicates that their relationships remain unresolved.

DISCUSSION

Comparison of Heterodontidae and †Paracestracionidae

Cladistic analysis and comparison of dental and non-dental features between *Heterodontus* and †*Paracestracion* supports the necessity for a family – †Paracestracionidae – to include all extinct forms of the latter.

Post-cranial features. Our findings emphasize the differences in body morphology between Heterodontidae and †Paracestracionidae and characterizes the latter as having pelvic fins that are placed more anterior as well as a first dorsal fin that is placed more posterior – two key features that are possessed by slow swimming epibenthic and benthic sharks (Figs 5, 6; Maia *et al.* 2012). In contrast, traits that are generally associated with a more active lifestyle, such as a (1) first dorsal fin and associated fin spine that are placed more anterior (2) pelvic girdle and fins that are placed more posterior and (3) pectoral girdle that is placed more anterior, are most clearly manifested in the Heterodontidae. The Late Jurassic culminated in a radiation in teleosts (Arratia 2004) as well as marine transgressions and minor mass extinctions that primarily affected coastal reef habitats (Hallam 1981, 1990, 2001; Moore & Ross 1994), which would have led to an increase in competition; it is plausible that the body morphology of *Heterodontus* contributed to their persistence into the Cretaceous, unlike *Paracestracion*.

†*Paracestracion* has previously been defined by the position of the pelvic fins, whereby they abut the pectorals and sit below the first dorsal fin (Kriwet *et al.* 2009*b*). Interestingly, the first dorsal fin spine's position along the vertebral column unambiguously distinguishes †*P. falcifer* and †*P. danieli.* Although this is also an autapomorphic character for †*P. viohli* sexual dimorphism cannot be ruled out (compare Daniel 1915) due to its missing posterior end and is therefore only characterized by its dental ornamentation in this study. Further, †*P. falcifer* (the holotype) and †*P. danieli* possess thorns. This trait, however, is also present in †*H. zitteli* and similar structures present in juvenile angel sharks are lost as they age (Compagno 2001). Investigation of the presence/absence of dorsal thorns in undoubtedly adult heterodontiforms is thus necessary to determine if it is an ontogenetic or a homoplastic feature.

Dentition. This study identifies an additional key characteristic of †Paracestracionidae to those of previous studies (Kriwet *et al.* 2009*b*): teeth exhibit a root shelf whereas in Heterodontidae the root lobes meet in the midline of the tooth and form a lingual protuberance. Additionally, the rate at which the number of cusps is reduced throughout ontogeny in extant Heterodontidae is very gradual when compared to †Paracestracionidae (Reif 1976; Fig. 3). The Meckel's cartilage and palatoquadrate in extant juveniles contains 13–17 and 17–21 tooth families, respectively (Reif 1976), while †*P. danieli* possesses 21 and 23 families, respectively, and the holotype for †*P. falcifer* possesses 29 on the palatoquadrate: this may indicate a major difference in feeding ecology between Heterodontidae and †Paracestracionidae (Slater 2016). Further studies on the ontogeny of heterodonty in Heterodontiformes, however, are required to confidently determine differences in dentition between the two families and examine the impact on their evolutionary fates.

Taxonomy of Heterodontiformes

Extant species of *Heterodontus* are divided into two groups based on tooth morphology (Reif 1976): following this concept, Hovestadt (2018) revises extant and extinct heterodontiform systematics and assigns fossil species to either morphotype 1 or 2 (corresponding to the Portusjacksoni and Francisci group, respectively, of Reif 1976 for extant species) or, if a combination of characters is present, to a new genus. New genera based exclusively on isolated fossil teeth were thus introduced: †*Protoheterodontus* is represented by a single occurrence from the Campanian (Late Cretaceous) of France (Guinot *et al.* 2013), †*Palaeoheterodontus* by a species in the late Late to early Middle Jurassic and †*Procestracion* by a single anterior tooth from the Kimmeridgian of southern Germany (Hovestadt 2018). Further, Hovestadt (2018) assumes †*Cestracion zitteli* to be undiagnosable (*nomina nuda*) due to an absence of preserved dentition and considers †*P. viohli* Kriwet, 2008 as a non-heterodontiform due to the lack of associated dental characters (p. 90). However, in this study, we show that – in addition to dental features – non-dental characters clearly identify †*Paracestracion zitteli* to represent the most basal member of heterodontids and support the inclusion of †*P. viohli* in †Paracestracionidae. Ultimately, systematic assignment of heterodontiforms based on dental characters alone is likely to provide ambiguous results due to an absence of data on the ontogeny of heterodonty as well as the prevalence of convergent evolution in elasmobranch dentition. Our study utilizes non-dental features to distinguish several species within the Heterodontiformes and thus highlights the importance of these characters in taxonomic analyses of heterodontiform fossils.

A new Super Order (Paracestrationiformes) and family (Paracestrationidae) was proposed (Jacques and Van Waes 2012) to include all members of the †*Paracestracion* genus however neither was registered. Our study confirms the necessity for the family †Paracestracionidae however we refrain from introducing a new order to include the †Paracestracionidae family due to the restriction of taxa in our analyses, which does not reject the interpretation that both families represent sister groups within Heterodontiformes.

Diversity patterns of heterodontiforms

A 1.7% decrease in species across the Jurassic/Cretaceous boundary is likely due to the limited number of species recorded in the Early Cretaceous, which may be a result of collecting bias: consequently, a significant decrease in heterodontiform diversity across the Jurassic/Cretaceous boundary cannot be unambiguously established. The Late Cretaceous heralds the highest species diversity in the evolutionary history of heterodontiforms however it is unbalanced among the epochs and is generally rather low.

Relationships within extant heterodontiforms

Origins of crown heterodontiforms. Divergence dates in this study are based on the minimum and maximum divergence dates between Rajiformes and Torpediniformes, which spans 187.8–209 Ma. Our estimate that crown heterodontiforms originated with *H. francisci* off the west coast of the Americas ca. 42.58 Ma largely supports a previous estimate of 47 Ma (Sorenson *et al.* 2014). *Heterodontus quoyi* (not included in this study) also occupies waters off the west coast of South America and was previously posited as the most plesiomorphic heterodontid due to the proximity of the anal fin to the caudal fin – as in †*H. zitteli* (Maisey 1982). It is therefore critical to obtain molecular information for *H. quoyi* to elucidate the origin of crown heterodontiforms.

Ultimately, our molecular phylogeny suggests that pre-Eocene – and especially Cretaceous heterodontiforms – represent stem group members. This contrasts with Hovestadt (2018), in which (apart from the absence of morphotype 2 from the Oligocene) both dental morphotypes are present in the Palaeogene, Neogene and the Late Cretaceous (Table 1). If dentitions bear not only a taxonomic but also a phylogenetic signal – which remains to be tested – this would indicate that species resembling modern heterodontiforms evolved in the late Early Cretaceous. Our results are, nevertheless, consistent with the data from Hovestadt (2018) that indicate that morphotype 2 (Francisci group of Reif 1976) is the most plesiomorphic of heterodontiform dentitions. We, however, consider the reconstruction of heterodontid evolution based on dental features alone insufficient: molecular information combined with morphological evidence from complete fossil specimens provides a larger, more robust dataset than one based on dental morphology.

Eastern Pacific species. During the mid-Eocene shallow waters of the Tethys Sea extended to what are presently the west coasts of the Americas, the east coast of North America and the Gulf of Mexico and the disparity in the oceanic temperature from the equator to the poles was reduced (Barron 1987; Sluijs *et al.* 2006; Hines *et al.* 2017): these conditions may have contributed to the migration and subsequent speciation of heterodontids during the mid-Eocene due to their strong preference for waters over 21 ^{o}C (Compagno 2001).

Western Pacific species. Results also reveal a monophyletic relation for species along the east Asiatic and Australian coasts (*H. zebra*, *H. portusjacksoni* and *H. galeatus*): future palaeontological discoveries might clarify the migration routes resulting in the divergence of these species (as well as those not included in this study along the east coast of Saudi Arabia and Africa) from those in the Eastern Pacific ca. 9.22 Ma (Ebert *et al.* 2017; Pollom *et al.* 2019). The topology of Western Pacific species in our phylogeny is likely different from that of Naylor *et al.* (2012) due to their use of Bayesian principles: further, the positions of *H. portusjacksoni* and *H. galeatus* are considered unresolved here.

CONCLUSIONS

Anatomical characters from complete bullhead shark fossils support the monophyly of Heterodontiformes, which can be separated into two families: one including solely extinct forms of †*Paracestracion* – assigned to †Paracestracionidae – and both extinct and extant forms of *Heterodontus* within the Heterodontidae. Although we recognize the importance of tooth morphologies in taxonomic analyses the phylogenetic signal of heterodontiform dental characters requires further investigation. This study emphasizes the importance of using non-dental features to provide a greater number of informative characters when investigating the systematics of chondrichthyan fossils.

Molecular phylogenetic analysis reveals that crown heterodontiforms likely originated off the west coast of the Americas due to a diversification event during the mid-Eocene. Further research, however, is required to elucidate the evolutionary history of Heterodontiformes and to clarify migration routes that led to the current distribution of *Heterodontus*.

Acknowledgements. We are grateful for the Palaeontological Association Undergraduate Research Bursary PA-UB201606 that financially supported T.S. on this project. We thank B. Pohl (Wyoming Dinosaur Center), P. Bartsch and J. Klapp (Museum für Naturkunde Berlin) and E. Bernard (London Natural History Museum) for access and assistance with their collections and G. Cuny for useful comments on the manuscript.

DATA ARCHIVING STATEMENT

Data for this study are available in the Dryad Digital Repository: https://datadryad.org/review?doi=doi:10.5061/dryad.6p4f83q

This published work and the nomenclatural act it contains, have been registered in ZooBank: http://zoobank.org/References/XXXXXXXXX

REFERENCES

AGNARSSON, I. and MILLER, J. A. 2008. Is ACCTRAN better than DELTRAN? *Cladistics*, **24**, 1–7.

ANDREEV, P. S., COATES, M. I., SHELTON, R. M., COOPER, P. R., SMITH, M. P., SANSOM and SANSOM, I. J. 2015. Upper Ordovician chondrichthyan-like scales from North America. *Palaeontology*, **58**, 691–704.

ARRATIA, G. 2004. Mesozoic halecostomes and the early radiation of teleosts. 279–315. *In* ARRATIA, G. and TINTORI, A. (eds,). *Mesozoic Fishes 3 – Systematics, Paleoenvironments and Biodiversity.* Dr Friedrich Pfeil Verlag, München, 649 pp.

ASCHLIMAN, N. C., NISHIDA, M., MIYA, M., INOUE, J. G., ROSANA, K. M., NAYLOR, G. J. 2012. Body plan convergence in the evolution of skates and rays (Chondrichthyes: Batoidea). *Molecular Phylogenetics and Evolution,* **63**, 28–42.

BARRON, E. J. 1987. Eocene equator-to-pole surface ocean temperatures: a significant climate problem? *Palaeoceanography,* **2**, 729–739.

BERG, L. S. 1940. Classification of fishes both recent and fossil. *Travaux de l'Institut Zoologique de l'Académie des Sciences de l'U.R.S.S.*, **5**, 85–517.

BONAPARTE, C. L. J. L. 1838. Selachorum tabula analytica. *Nuovi Annali Scienze Naturali,* **2**, 195–214.

CARVALHO, M. R. and MAISEY, J. G. 1996. Phylogenetic relationships of the Late Jurassic shark Protospinax WOODWARD 1919 (Chondrichthyes: Elasmobranchii). 9–46. *In* ARRATIA, G., VIOHL, G. (eds.). *Mesozoic fishes 1 - systematics and paleoecology.* Dr Friedrich Pfeil Verlag, München, Germany, 576 pp.

COMPAGNO, L. J. V. 1973. Interrelationships of living elasmobranches. 15–61. *In* GREENWOOD, P. H., MILES, R. S. and PATTERSON, C. (eds.). *Interrelationships of fishes*. Linnean Society of London, London*,* 536 pp.

— 1977. Phyletic relationships of living sharks and rays. *Integrative and Comparative Biology,* **17**, 303–322.

— 2001. Sharks of the world: an annotated and illustrated catalogue of shark species known to date*. Volume 2. Bullhead, Mackerel and Carpet sharks (Heterodontiformes, Lamniformes and Orectolobiformes)*. Food and Agriculture Organization of the United Nations, Rome, 269 pp.

CUNY, G. and BENTON, M. J. 1999. Early radiation of the Neoselachian sharks in Western Europe. *GEOBIOS*, **32**, 193–204.

DANIEL, J. F. 1915. The anatomy of *Heterodontus francisci*. II. The endoskeleton. *Journal of Morphology,* **26**, 447–493.

EBERT, D. A., KHAN, M., VALINASSAB, T., AKHILESH, K. V. and TESFAMICHAEL, D. 2017. *Heterodontus omanensis. The IUCN Red List of Threatened Species.* <http://dx.doi.org/10.2305/IUCN.UK.2017-2.RLTS.T161720A109916524.en>. Downloaded on 18 June 2018.

FELSENSTEIN, J. 1985. Confidence limits on phylogenies: an approach using the bootstrap. *Evolution*, **39**, 783–791.

GUINOT, G. and CAVIN, L. 2015. Contrasting “fish” diversity dynamics between marine and freshwater environments. *Current Biology,* **25**, 2314–2318.

— UNDERWOOD, C., CAPPETTA, H. and WARD, D. 2013. Sharks from the Late Cretaceous of France and the U.K. *Journal of Systematic Palaeontology*, **11**, 589–671.

HALLAM, A. 1981. The End-Triassic bivalve extinction event. *Palaeogeography, Palaeoclimatology, Palaeoecology,* **35**, 1–44.

— 1990. The end-Triassic mass extinction event. 577–583. *In* SHARPTON, V. L. and WARD, P. D. (eds.). *Global catastrophes in Earth history: An interdisciplinary conference on impacts, volcanism, and mass mortality. Geological Society of America Special Paper* **247**, 644 pp.

— 2001. A review of the broad pattern of Jurassic sea-level changes and their possible causes in the light of current knowledge. *Palaeogeography, Palaeoclimatology, Palaeoecology,* **167**, 23–37.

HAMMER, Ø., HARPER, D. A. T. and RYAN, P. D. 2001. PAST: Palaeontological Statistics software package for education and data analysis. *Palaeontologia Electronica*, **4**, 1–9.

HARVEY, P. H. and PAGEL, M. D. 1991. *The comparative method in evolutionary biology.* Oxford Series in Ecology and Evolution. Oxford University Press, New York, 248 pp.

HAY, O. P. 1902. Bibliography and catalogue of the fossil Vertebrata of North America. *Bulletin of the United States Geological Survey,* **179**, 1–868.

HINES, B. R., HOLLIS, C. J., ATKINS, C. B., BAKER, J. A., MORGANS, H. E. G. and STRONG, P. C. 2017. Reduction of oceanic temperature gradients in the early Eocene Southwest Pacific Ocean. *Palaeogeography, Palaeoclimatology, Palaeoecology,* **475**, 41–54.

HOVESTADT, D. C. 2018. Reassessment and revision of the fossil Heterodontidae (Chondrichthyes: Neoselachii) based on tooth morphology of extant taxa. *Palaeontos*, **30**, 3–120.

HUMAN, B. A., OWEN, E. P., COMPAGNO, L. J., V. and HARLEY, E. H. 2006. Testing morphologically based phylogenetic theories within the cartilaginous fishes with molecular data, with special reference to the catshark family (Chondrichthyes; Scyliorhinidae) and the interrelationships within them. *Molecular Phylogenetics and Evolution,* **39**, 384–391.

HUXLEY, T. H. 1880. On the application of the laws of evolution to the arrangement of the Vertebrata and more particularly of the Mammalia. *Proceedings of the Zoological Society of London,* **43**, 649–662.

INOUE, J. G., MIYA, M., LAM, K., TAY, B. H., DANKS, J. A., BELL, J., WALKER, T. I., VENKATESH, B. 2010. Evolutionary origin and phylogeny of the modern holocephalans (Chondrichthyes: Chimaeriformes): a mitogenomic perspective. *Molecular Biology and Evolution,* **27**, 2576–2586.

JACQUES, H., VAN WAES, H. 2012. Observations Concerning the Evolution and the Parasystematic of all the living and fossil Heterodontiformes. *Géominpal Belgica,* **3**, 1–17.

KLUG, S. 2010. Monophyly, phylogeny and systematic position of the †Synechodontiformes (Chondrichthyes, Neoselachii). *Zoological Scripta,* **39**, 37–49.

KOKEN, E. 1911. Pisces. *In* ZITTEL, K. A. (ed.). *Grundzüge der Paläontologie. Volume 2.* München, Berlin, Oldenbourg, 142 pp.

KRIWET, J. 2008. A new species of extinct bullhead sharks, *Paracestracion viohli* (Neoselachii, Heterodontiformes), from the Upper Jurassic of South Germany. *Acta Geologica Polonica*, **58**, 235–241.

— and KLUG, S. 2004. Late Jurassic selachians (Chondrichthyes, Elasmobranchii) from southern Germany: Re-evaluation on taxonomy and diversity. *Zitteliana*, **A44**: 67-95.

— and KLUG, S. 2008. Diversity and biogeography patterns of Late Jurassic neoselachians (Chondrichthyes: Elasmobranchii). 55–70. *In* LONGBOTTOM, A. E.

and RICHTER, M. (eds). *Fishes and the Break-up of Pangaea.* Special Publications of the Geological Society, London, 372 pp.

— KIESSLING, W. and KLUG, S. 2009*a*. Diversification trajectories and evolutionary life-history traits in early sharks and batoids. *Proceedings of the Royal Society, Series B,* **276**, 945–951.

— NUNN, E. V. and KLUG, S. 2009*b*. Neoselachians (Chondrichthyes, Elasmobranchii) from the Lower and lower Upper Cretaceous of north-eastern Spain. *Zoological Journal of the Linnean Society,* **155**, 316–347.

KUMAR, S., STECHER, G. and TAMURA, K. 2016. MEGA7: Molecular Evolutionary Genetics Analysis version 7.0 for bigger datasets. *Molecular Biology and Evolution*, **33**, 1870–1874.

MADDISON, W. P. and MADDISON, D. R. 2018. Mesquite: a modular system for evolutionary analysis. Version 3.51. <http://www.mesquiteproject.org>

MAIA, A. M. R., WILGA, C. A. D. and LAUDER, G. V. 2012. Biomechanics of locomotion in sharks, rays, and chimeras. 125–151. *In* CARRIER, J. C., MUSICK, J. A. and HEITHAUS, M. R. (eds.). *Biology of Sharks and Their Relatives II: Biodiversity, Adaptive Physiology, and Conservation*. CRC Press Taylor & Francis Group, Boca Raton, Florida, 666 pp.

MAISEY, J. G. 1982. Fossil Hornshark Finspines (Elasmobranchii; Heterodontidae) with Notes on a New Species (*Heterodontus tuberculatus*). *Neues Jahrbuch für Geologie und Paläontologie, Abhandlungen,* **164**, 393–413.

— 2012. What is an 'elasmobranch'? The impact of palaeontology in understanding elasmobranch phylogeny and evolution. *Journal of Fish Biology*, **80**, 918–951.

— NAYLOR, G. J. P. and WARD, D. J. 2004. Mesozoic elasmobranchs, neoselachian phylogeny and the rise of modern elasmobranch diversity. 17–56. *In* ARRATIA, G. and TINTORI, A. (eds,). *Mesozoic Fishes 3 – Systematics, Paleoenvironments and Biodiversity.* Dr Friedrich Pfeil Verlag, München, 649 pp.

MALLATT, J. and WINCHELL, C. J. 2007. Ribosomal RNA genes and deuterostome phylogeny revisited: more cyclostomes, elasmobranchs, reptiles, and a brittle star. *Molecular Phylogenetics and Evolution,* **43**, 1005–1022.

MOORE, G. T. and ROSS, C. A. 1994. Kimmeridgian-Tithonian (Late Jurassic) dinosaur and ammonoid paleoecology from a paleoclimate simulation. *Canadian Society of Petroleum Geologists Memoir*, **17**, 345–361.

NAYLOR, G. J. P., CAIRA, J. N., JENSEN, K. R. E., ROSANA, K. M., STRAUBE, N. and LAKNER, C. 2012. Elasmobranch phylogeny: a mitochondrial estimate based on 595 species. 31–56. *In* CARRIER, J. C., MUSICK, J. A. and HEITHAUS, M. R. (eds.). *Biology of Sharks and Their Relatives II: Biodiversity, Adaptive Physiology, and Conservation*. CRC Press Taylor & Francis Group, Boca Raton, Florida, 666 pp.

POLLOM, R., BENNETT, R., EBERT, D. A., FERNANDO, S., JABADO, R. W., KUGURU, B., SAMOILYS, M. 2019. *Heterodontus ramalheira. The IUCN Red List of Threatened Species.* < http://dx.doi.org/10.2305/IUCN.UK.2019-2.RLTS.T44614A140353520.en. Downloaded on 05 August 2019.

POWTER, D. 2007. Conservation biology of the Port Jackson shark, *Heterodontus portusjacksoni*, in New South Wales. Unpublished PhD thesis*,* University of Newcastle, Australia, 466 pp.

REIF, W. -E. 1976. Morphogenesis, pattern formation and function of the dentition of *Heterodontus* (Selachii). *Zoomorphologie*, **83**, 1–47.

SLATER, T. 2016. Sharks with question marks – impacts of a new fossil on interrelationships of early bullhead sharks. 68–72. *In* McNAMARA, M. E. (ed.). *Palaeontology Newsletter.* The Palaeontological Association, Durham, 88 pp.

— ASHBROOK, K. and KRIWET, J. 2019. Evolutionary relationships among bullhead sharks (Chondrichthyes: Heterodontiformes). *Dryad Digital Repository.* https://doi.org/10.5061/dryad.6p4f83q

SLUIJS, A., SCHOUTEN, S., PAGANI, M., WOLTERING, M., BRINKHUIS, H., DAMSTÈ, J. S. S., DICKENS, G. R., HUBER, M., REICHART, G. -J., STEIN, R., MATTHIESSEN, J., LOURENS, L. J., PEDENTCHOUK, N., BACKMAN, J., MORAN,

K. and EXPEDITION 302 SCIENTISTS. 2006. Subtropical Arctic Ocean temperatures during the Palaeocene/Eocene thermal maximum. *Nature,* **441**, 610–613.

SORENSON, L., SANTINI, F. and ALFARO, M. E. 2014. The effect of habitat on modern shark diversification. *Journal of Evolutionary Biology,* **27**, 1536–1548.

STRONG, W. R., Jr. 1989. Behavioral ecology of horn sharks, *Heterodontus francisci*, at Santa Catalina Island, California, with emphasis on patterns of space utilization. Unpublished MSc thesis, California State University, California, USA.

SWAFFORD, D. L. 2002. PAUP*. Phylogenetic Analysis Using Parsimony (*and other methods). Version 4. Sinauer Associates, Sunderland, Massachusetts.

THIES, D. 1983. Jurazeitliche Neoselachier aus Deutschland und S-England (Jurassic Neoselachians from Germany and S-England). *Courier Forschunginstitut Senckenberg,* **58**, 1–116.

TYTELL, E. D. 2006. Median fin function in bluegill sunfish *Lepomis macrochirus*: streamwise vortex structure during steady swimming. *Journal of Experimental Biology,* **209**, 1516–34.

WAGNER, J. A. 1857. Charakteristik neuer Arten von Knorpelfischen aus den lithographischen Schiefern der Umgegend von Solnhofen. *Gelehrte Anzeigen der königlich bayerischen Akademie der Wissenschaften,* **44**, 288–293.

WINCHELL, C. J., MARTIN, A. P. and MALLATT, J. 2004. Phylogeny of elasmobranchs based on LSU and SSU ribosomal RNA genes. *Molecular Phylogenetics and Evolution,* **31**, 214–224.

FIGURES

FIG. 1. Geological map of Eichstätt, Germany and surrounding areas. Stars indicate locality from which †*Paracestracion danieli* was excavated.

FIG. 2. Photographs of †*Paracestracion danieli*, a complete fossil subadult heterodontiform. A, UV image. B, counterpart. C, palatoquadrate and Meckel's cartilage with teeth in situ. D, anterior tooth. E, parasymphysial tooth. F, lateral teeth. G, root vascularization of anterior teeth. H, rostral denticles. I, cranial denticles. J, ventral denticles. K, denticles on leading edge of pelvic fin. Scale bars represent: 1 cm (A–C); 0.5 mm (D–K).

FIG. 3. A, anterior dorsal fin spine. B, posterior dorsal fin spine. C, dorsal denticles. D, dorsal thorn. Scale bars represent: 1 mm (A–B); 0.5 mm (C–D).

FIG. 4. Tooth morphology of anterior teeth throughout ontogeny for †extinct and extant heterodontids. The darker grey region denotes the tooth root for †*P. falcifer*. Adapted from Reif (1976). All scale bars represent 1 mm.

FIG 5. PCA of allometrically scaled distance measurements taken from extinct and extant heterodontids. Ellipses, 95% confidence interval. Adapted from Slater (2016).

FIG 6. Morphometric cladogram of extinct and extant heterodontids. Labels on nodes indicate bootstrap estimates for ACCTRAN and DELTRAN optimization (the latter in bold). Crosses indicate extinct species. TL, total length; RI, retention index; CI, consistency index.

FIG 7. A molecular, maximum likelihood phylogeny of extant Heterodontiformes. Bootstrap values and divergence times are indicated (the latter in bold).

TABLE 1. Standing diversity of extinct and extant heterodontiforms through time. Raw data and stratigraphic information taken from Reif (1976) and Hovestadt (2018) are presented with respect to the authors' proposed dental morphotypes. CI, confidence interval; N, number of species.

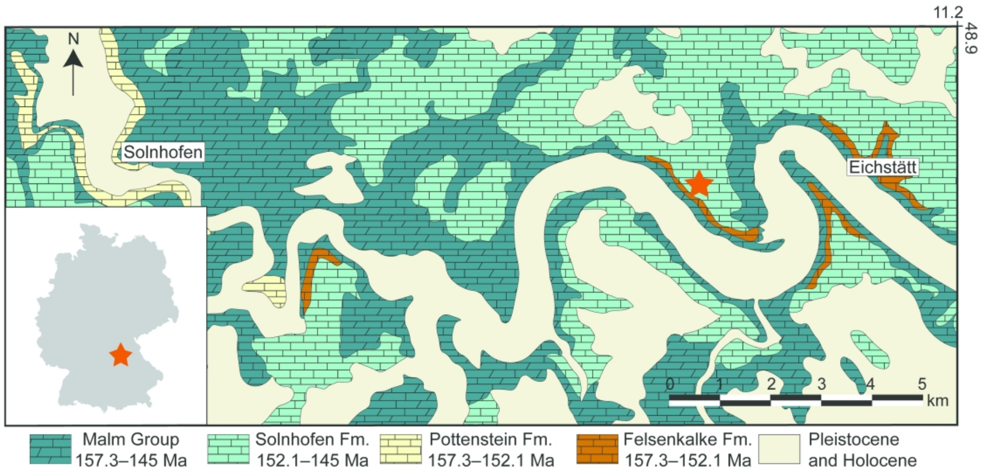

FIG. 1. Geological map of Eichstätt, Germany and surrounding areas. Stars indicate locality from which †Paracestracion danieli was excavated.

160x75mm (600 x 600 DPI)

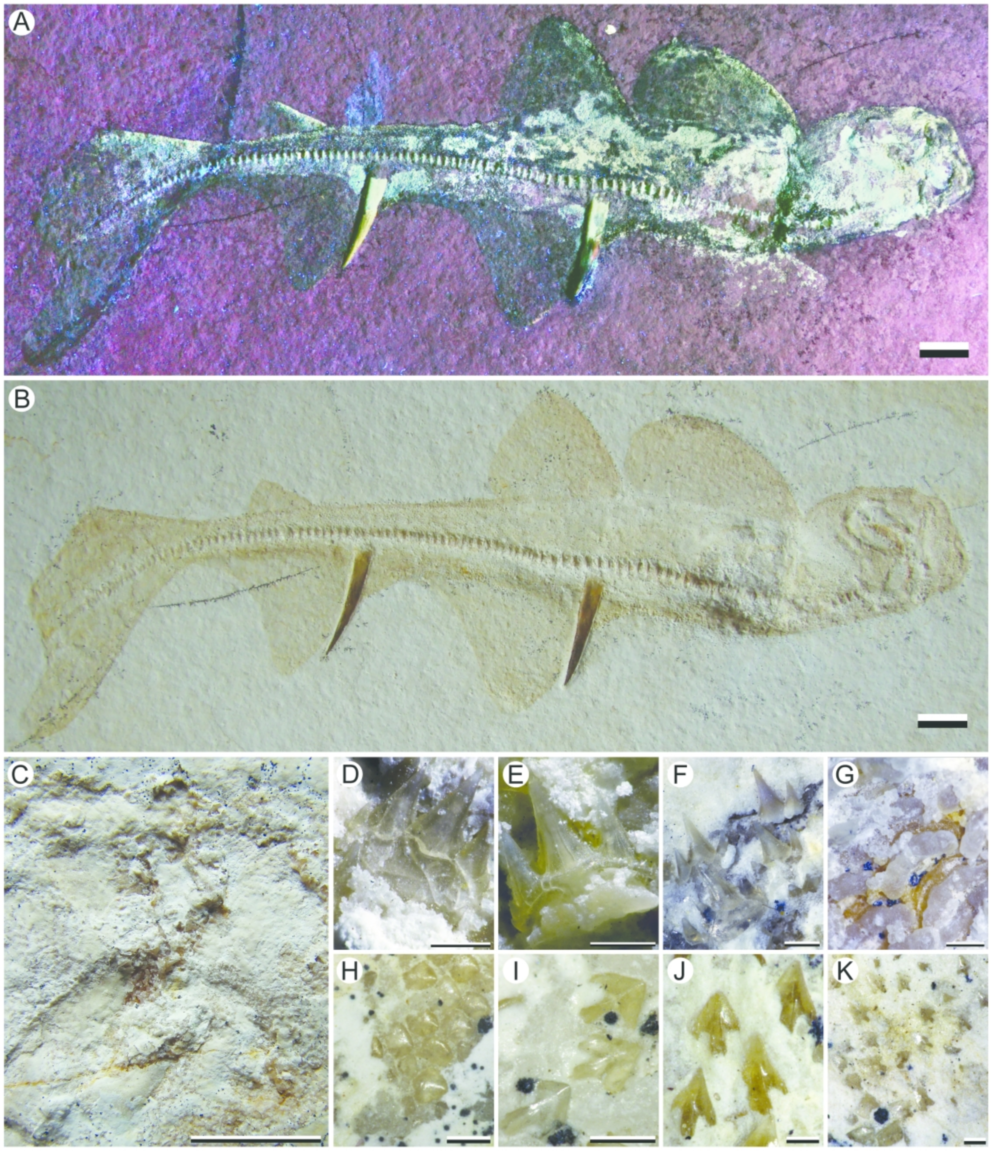

FIG. 2. Photographs of †Paracestracion danieli, a complete fossil subadult heterodontiform. A, UV image. B, counterpart. C, palatoquadrate and Meckel's cartilage with teeth in situ. D, anterior tooth. E, parasymphysial tooth. F, lateral teeth. G, root vascularization of anterior teeth. H, rostral denticles. I, cranial denticles. J, ventral denticles. K, denticles on leading edge of pelvic fin. Scale bars represent: 1 cm (A–C); 0.5 mm (D–K).

160x185mm (600 x 600 DPI)

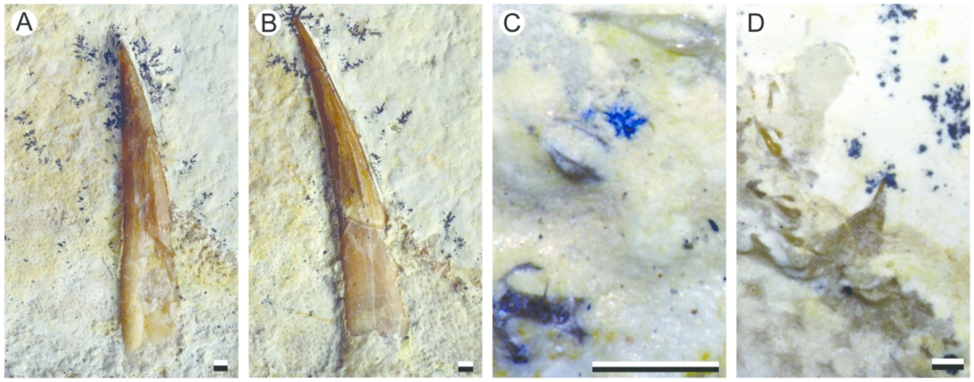

FIG. 3. A, anterior dorsal fin spine. B, posterior dorsal fin spine. C, dorsal denticles. D, dorsal thorn. Scale bars represent: 1 mm (A–B); 0.5 mm (C–D).

160x62mm (600 x 600 DPI)

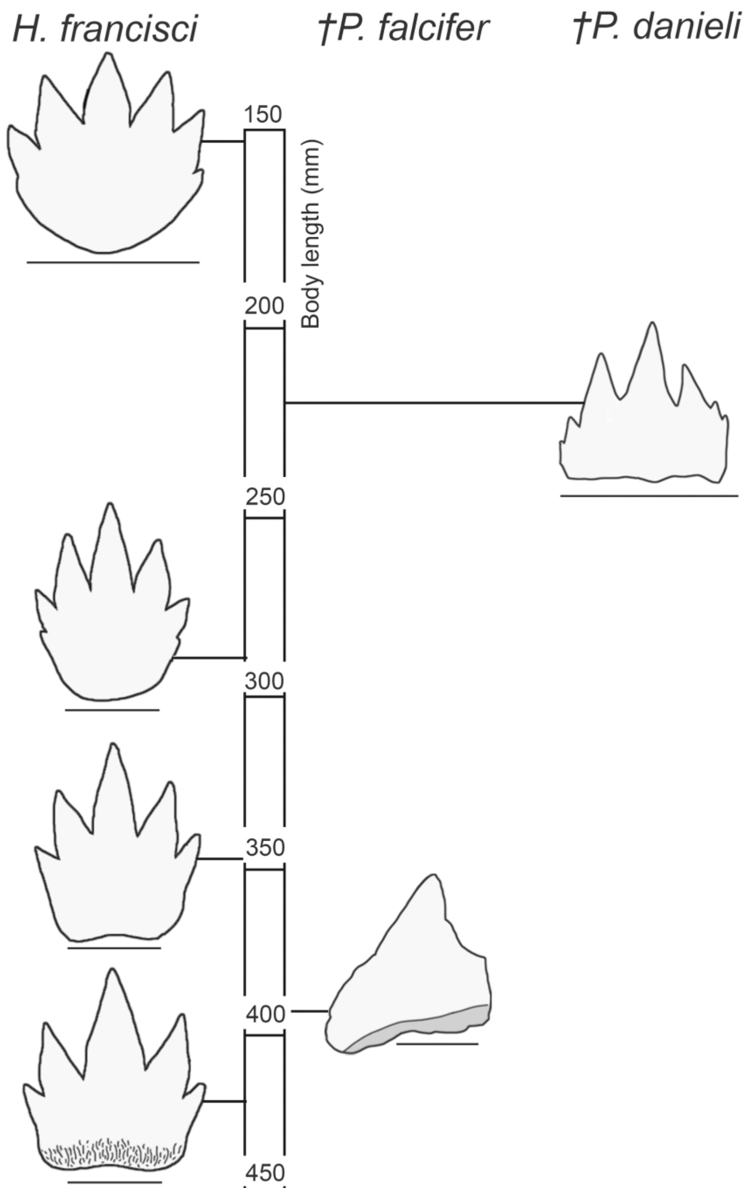

FIG. 4. Tooth morphology of anterior teeth throughout ontogeny for †extinct and extant heterodontids. The darker grey region denotes the tooth root for †P. falcifer. Adapted from Reif (1976). All scale bars represent 1 mm.

80x115mm (600 x 600 DPI)

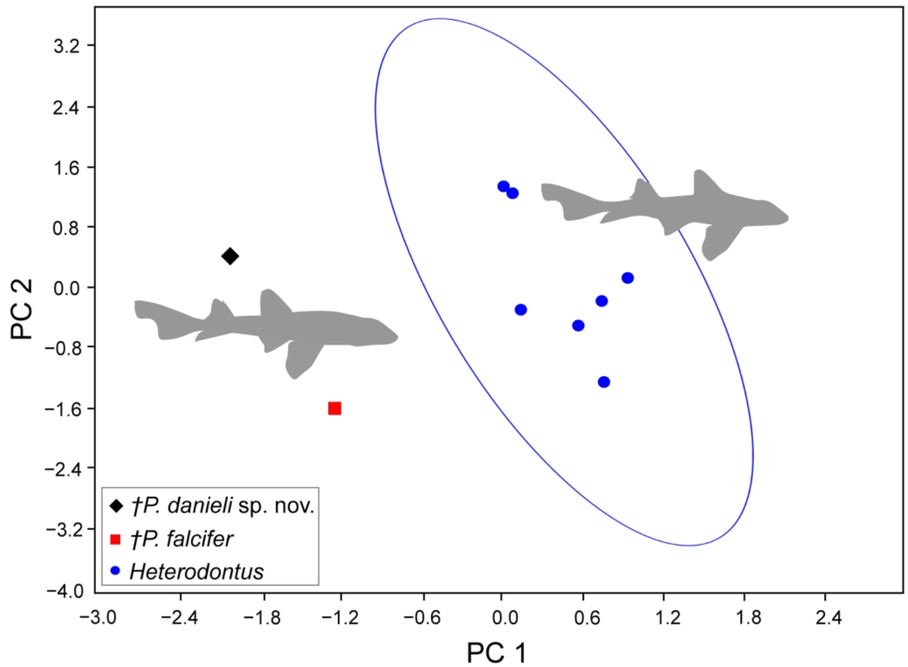

FIG 5. PCA of allometrically scaled distance measurements taken from extinct and extant heterodontids. Ellipses, 95% confidence interval. Adapted from Slater (2016).

109x75mm (600 x 600 DPI)

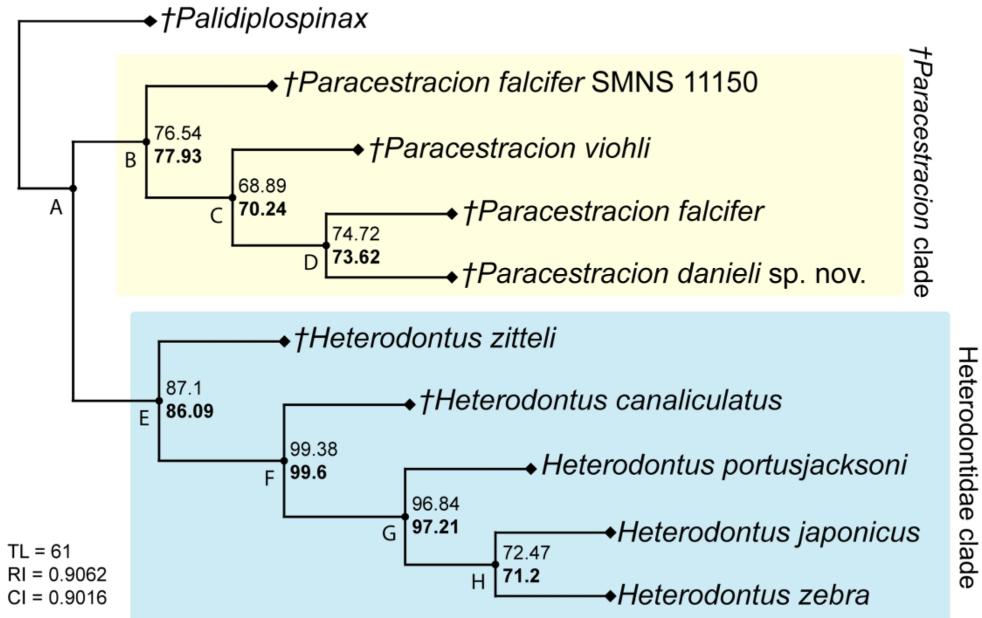

FIG 6. Morphometric cladogram of extinct and extant heterodontids. Labels on nodes indicate bootstrap estimates for ACCTRAN and DELTRAN optimization (the latter in bold). Crosses indicate extinct species. TL, total length; RI, retention index; CI, consistency index.

110x75mm (600 x 600 DPI)

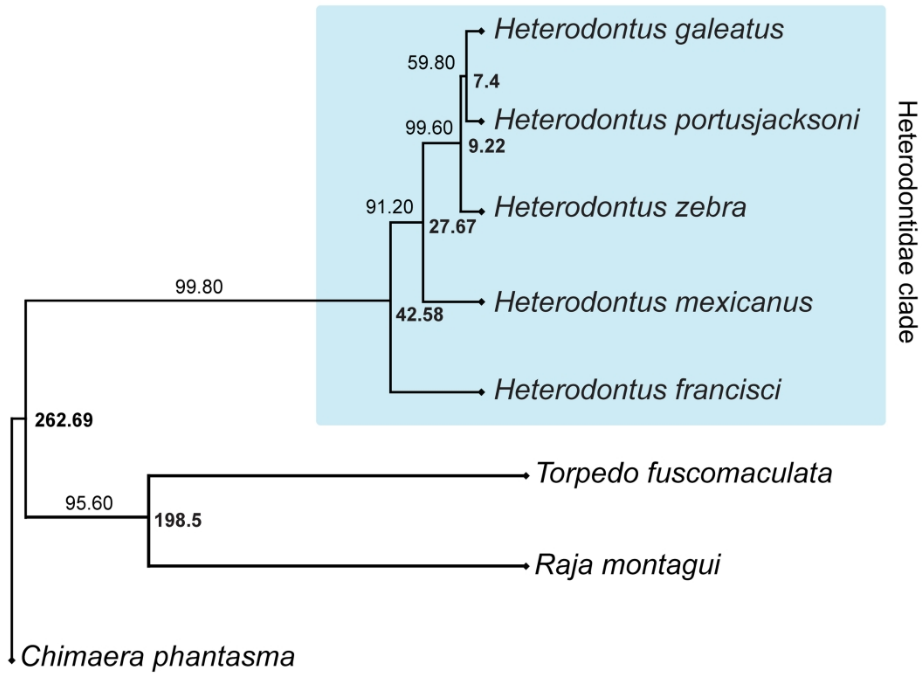

FIG 7. A molecular, maximum likelihood phylogeny of extant Heterodontiformes. Bootstrap values and divergence times are indicated (the latter in bold).

110x75mm (600 x 600 DPI)

	Morphotype			N		Total species (%)	Upper and lower limits of 95% CI (%)
	1	**2**	**?**	**Epoch**	**Series**		
Recent	3	6		9	9	15.8	-8.98/+10.05
Pliocene	1	1		2	7	12.3	-7.82/+9.19
Miocene	1	4		5			
Oligocene	1			1	10	17.5	-9.33/+10.46
Eocene	4	3		7			
Palaeocene	1	1		2			
Maastrichtian	1	1	2	3	15	26.3	-11.06/+11.84
Campanian	1			1			
Santonian	1			1			
Coniacian							
Turonian		1		1			
Cenomanian	4	4	1	9			
Aptian/Albian		1	1	2	5	8.8	-6.72/+7.97
Barremian			1	1			
Hauterivian							
Valanginian			2	2			
Berriasian							
Late Jurassic				6	6	10.5	-7.37/+8.67
Middle Jurassic				4	4	7	-5.89/+7.39
Early Jurassic				1	1	1.8	-5.89/+7.39
Total species					**57**		